Inhibition of Microglia Over-activation Restores Neuronal Survival in a Mouse Model of CDKL5 Deficiency Disorder

Giuseppe Galvani
University of Bologna: Universita di Bologna
Nicola Mottolese
University of Bologna: Universita di Bologna
Laura Gennaccaro
University of Bologna: Universita di Bologna
Manuela Loi
University of Bologna: Universita di Bologna
Giorgio Medici
University of Bologna: Universita di Bologna
Marianna Tassinari
University of Bologna: Universita di Bologna
Claudia Fuchs
University of Bologna: Universita di Bologna
Elisabetta Ciani
University of Bologna: Universita di Bologna
Stefania Trazzi (stefania.trazzi3@unibo.it)
University of Bologna: Universita di Bologna https://orcid.org/0000-0003-2623-2769

Research

Keywords: CDKL5, neuroinflammation, neuronal survival, luteolin

Posted Date: February 17th, 2021

DOI: https://doi.org/10.21203/rs.3.rs-203260/v1

Version of Record: A version of this preprint was published at Journal of Neuroinflammation on July 8th, 2021. See the published version at https://doi.org/10.1186/s12974-021-02204-0.

Abstract

Background

CDKL5 Deficiency Disorder (CDD), a severe neurodevelopmental disorder characterized by early-onset epilepsy, intellectual disability, and autistic features, is caused by mutations in the *CDKL5* gene. Evidence in animal models of CDD showed that absence of CDKL5 negatively affects neuronal survival, as well as neuronal maturation and dendritic outgrowth; however, knowledge of the substrates underlying these alterations is still limited. Neuro-inflammatory processes are known to contribute to neuronal dysfunction and death. Recent evidence shows a subclinical chronic inflammatory status in plasma from CDD patients. However, to date, it is unknown whether a similar inflammatory status is present in the brain of CDD patients and, if so, whether this plays a causative or exacerbating role in the pathophysiology of CDD.

Methods

We evaluated microglia activation using AIF-1 immunofluorescence, proinflammatory cytokine expression and signaling in the brain of a mouse model of CDD, the *Cdkl5* KO mouse, which is characterized by an impaired survival of hippocampal neurons that worsens with age. Hippocampal neuron survival was determined by DCX, NeuN and cleaved caspase-3 immunostaining in *Cdkl5* KO mice treated with luteolin (10 mg/kg), a natural anti-inflammatory flavonoid. Since hippocampal neurons of *Cdkl5* KO mice exhibit increased susceptibility to excitotoxic stress, we evaluated neuronal survival in *Cdkl5* KO mice injected with NMDA (60 mg/kg) after a 7-day treatment with luteolin.

Results

We found increased microglial activation in the brain of the *Cdkl5* KO mouse. We found alterations in microglial cell morphology and number, increased levels of AIF-1 and proinflammatory cytokines, and activation of STAT3 signaling. Remarkably, treatment with luteolin recovers microglia alterations as well as neuronal survival and maturation in *Cdkl5* KO mice, and prevents the increase in NMDA-induced cell death in the hippocampus.

Conclusions

Our results suggest that neuro-inflammatory processes contribute to the pathogenesis of CDD and imply the potential usefulness of luteolin as a treatment option in CDD patients.

Background

The cyclin-dependent kinase-like 5 gene (*CDKL5*), located on the short arm of the X-chromosome [1], encodes for a serine/threonine kinase that is highly expressed in the brain [2]. Genetic mutations of this gene cause absence of a functional CDKL5 protein, resulting in a severe neurodevelopmental encephalopathy named CDKL5 deficiency disorder (CDD; OMIM 300203, 300672). This disorder is

associated with early onset epilepsy, and severe cognitive, motor, visual, and sleep disturbances [3–5]. An animal model of CDD, the *Cdkl5* knockout (KO) mouse [6–9], recapitulates, to varying degrees, the underlying molecular and behavioral defects of the human disease. Interestingly, mouse models of CDD do not have recurrent epileptic seizures, but nonetheless demonstrate significant behavioral deficits: learning and memory, motor control and social interaction deficits, visual impairments, and sleep disturbances [6–14].

Changes in neuronal morphology such as dendritic branching and stability of dendritic spines have been consistently reported in *Cdkl5* KO mice [6, 7]. *Cdkl5* KO mice showed a reduction in dendritic length of cortical and hippocampal pyramidal neurons [6, 11, 15, 16] and changes in the maturation and stability of dendritic spines, as well as in the density of PSD-95 dendritic clusters in several brain structures [10, 15–18].

Interestingly, recent evidence has shown that CDKL5, in addition to neuronal maturation and dendritic outgrowth, also affects neuronal survival [11, 19, 20]. *Cdkl5* KO mice are characterized by an increased rate of apoptotic cell death in the hippocampal dentate gyrus that causes a reduction in the final number of granule neurons [11] and by accelerated neuronal senescence/death during aging [21]. Moreover, hippocampal neurons of *Cdkl5* KO mice exhibit increased susceptibility to neurotoxic/excitotoxic stress [19, 20], indicating that absence of Cdkl5 increase neuronal vulnerability.

Neuroinflammatory processes are known to contribute to neuronal dysfunction and death. When over-activated in response to neuronal damage and genetic or environmental factors, microglia, the brain macrophages [22], cause widespread damage to neighboring neurons. Indeed, reactive microglia kill neurons by producing neurotoxic factors and pro-inflammatory molecules such as tumor necrosis factor-α (TNF-α) and interleukin-1β and − 6 (IL-1β, IL-6) [23, 24]. Remarkably, over-activated microglia have been described in several neurodegenerative diseases such as Alzheimer's, Parkinson's, and Huntington's diseases and Amyotrophic lateral sclerosis [25–27], suggesting that active neuroinflammation may account for the compromised neuronal survival observed in these pathologies. Interestingly, active neuroinflammation could account for the compromised brain development observed in neurodevelopmental disorders such as Down syndrome, autism-spectrum disorders (ASD), and Rett syndrome [28–30], by damaging synaptic connectivity.

Recently, a major cytokine dysregulation proportional to clinical severity, inflammatory status, and redox imbalance was evidenced in plasma from CDD patients [31, 32], suggesting a subclinical chronic inflammatory status in children affected by this pathology. However, to date, it is unknown whether such an inflammatory state is even mirrored at the cerebral level and whether it can contribute to the pathophysiology of CDD.

Here, we show evidence of a microglia over-activation status in the brain of *Cdkl5* KO mice, characterized by alterations in microglia cell number/morphology and increased pro-inflammatory gene expression. We found that microglia over-activation is already present in the postnatal period in *Cdkl5* KO mice and worsens during aging. Importantly, by restoring microglia alterations, treatment with luteolin, a natural

anti-inflammatory flavonoid, counteracts hippocampal neuron cell death in both adult and aged *Cdkl5* KO mice, and rescues NMDA-induced excitotoxic damage in *Cdkl5* KO mice. These findings highlight new insights into the CDD pathophysiology and provide the first evidence that therapeutic approaches aimed at counteracting neuroinflammation could be beneficial in CDD.

Materials And Methods

Colony and husbandry

The mice used in this work derive from the *Cdkl5* null strain in the C57BL/6N background developed in [6] and backcrossed in C57BL/6J for three generations. Mice for experiments were produced by crossing *Cdkl5* +/− females with *Cdkl5* -/Y males and *Cdkl5* +/− females with +/Y males [6]; animals were karyotyped by PCR on genomic DNA as previously described [6] and littermate controls were used for all experiments. P0, postnatal day zero, was designated as the day of birth and 24 h later mice were considered 1-day-old animals (P1). Mice were housed three to five per cage and maintained in a temperature- (23 C) and humidity-controlled environment with a standard 12 h light/dark cycle, and provided with standard mouse chow and water *ad libitum*. Animals' day-to-day health and comfort were monitored by the veterinary service. All possible efforts were made to minimize suffering and the number of animals used. Experiments were carried out on a total of 89 *Cdkl5* KO mice (*Cdkl5* +/Y, n = 4; *Cdkl5* -/Y, n = 4; *Cdkl5* +/+, n = 26; *Cdkl5* +/-, n = 55).

Treatments

All treatments were performed in the animal house at the same hour of the day.

Luteolin treatment - The dose of luteolin was chosen based on [33]. Mice were intraperitoneally (i.p.) injected daily with saline or luteolin (10 mg/kg in saline; Tocris) for 7 or 20 days. The day following the last treatment mice were sacrificed for histological and Western blot analyses.

NMDA treatment - Mice were treated with an intraperitoneal injection of NMDA (60 mg/kg; Sigma-Aldrich) in phosphate-buffered saline (PBS) after 7 days of luteolin treatment. Animals were sacrificed 24 h or 8 days after NMDA injection and immunohistochemical analysis was assessed as described below.

TATκ-GFP-CDKL5 protein treatment – Brain sections processed for AIF-1 immunohistochemistry derived from animals used in [34]. Briefly, mice were treated twice a day (morning and evening) with TATκ-GFP or TATκ-GFP-CDKL5 protein (50 ng/injection) directly injected into the carotid artery through a programmable pump [34].

Histological and immunohistochemical procedures

Animals were anesthetized with 2% isoflurane (in pure oxygen) and sacrificed through cervical dislocation. Brains were quickly removed and cut along the midline. While right hemispheres were quickly frozen and used for Western blot analyses, left hemispheres were fixed via immersion in 4%

paraformaldehyde (100 mM phosphate buffer, pH 7.4) for 48 h, kept in 15–20% sucrose for an additional 24 h and then frozen with cold ice. Hemispheres were cut with a freezing microtome into 30 µm-thick coronal sections and processed for immunohistochemistry procedures as described below. Brain sections from *Emx1* KO mice used in [35] were processed for AIF-1 immunohistochemistry.

AIF-1, NeuN and Ki-67 immunohistochemistry - One out of every eight free-floating sections from the hippocampal formation was incubated with one of the following primary antibodies: rabbit polyclonal anti-AIF-1 antibody (1:300; ThermoFisher), mouse monoclonal anti-NeuN antibody (1:250; Merk Millipore), or rabbit monoclonal Ki-67 antibody (1:100; Thermoscientific). Sections were then incubated for 2 h at room temperature with a Cy3-conjugated anti-rabbit secondary antibody (1:200, Jackson ImmunoResearch Laboratories, Inc.) for AIF-1 and Ki-67 immunohistochemistry, and with a Cy3-conjugated anti-mouse secondary antibody (1:200, Jackson ImmunoResearch Laboratories, Inc.) for NeuN immunohistochemistry. Nuclei were counterstained with Hoechst-33342 (Sigma-Aldrich).

Cleaved caspase-3 staining - For cleaved caspase-3 immunofluorescence, one out of every six sections from the hippocampal formation was incubated overnight with a rabbit polyclonal anti-cleaved caspase-3 antibody (1:200; Cell Signaling Technology). The following day the sections were washed and incubated with an HRP-conjugated anti-rabbit secondary antibody (1:200; Jackson Immunoresearch, Inc.). Detection was performed using the TSA Cyanine 3 Plus Evaluation Kit (Perkin Elmer) and nuclei were counterstained with Hoechst 33342 (Sigma-Aldrich).

DCX immunohistochemistry - One out of every six free-floating sections from the hippocampal formation was incubated overnight with a goat polyclonal anti-doublecortin antibody (DCX, 1:1000, Santa Cruz Biotechnology, Inc.). The following day the sections were washed and incubated with a biotinylated anti-goat IgG secondary antibody (1:200, Vector BioLabs, Malver, PA, USA) for 2 h and thereafter for 1 h with the VECTASTAIN®ABC kit (Vector BioLabs). Detection was performed using DAB kit (Vector BioLabs).

Image acquisition and measurements

Fluorescence images were taken with an Eclipse TE 2000-S microscope equipped with a DS-Qi2 digital SLR camera (Nikon Instruments Inc.). A light microscope (Leica Mycrosystems) equipped with a motorized stage and focus control system and a color digital camera (Coolsnap-Pro; Media Cybernetics) were used for neuronal tracing and to take bright field images. Measurements were carried out using Image Pro Plus software (Media Cybernetics, Silver Spring, MD, USA).

Cell density - The number of AIF-1-positive cells in the hippocampus and somatosensory cortex was manually counted using the point tool of the Image Pro Plus software (Media Cybernetics, Silver Spring, MD, USA) and cell density was established as AIF-1-positive cells/mm^3. The density of Hoechst-positive nuclei, of neurons (NeuN-positive), and apoptotic cells (cleaved caspase-3-positive) in the CA1 layer were manually counted and expressed as cells/mm^3. Ki-67-positive cells were counted in the subgranular zone of the dentate gyrus, and expressed as number of cells/mm.

Morphometric microglial cell analysis – Starting from 20X magnification images of AIF-1-stained hippocampal and cortical slices, AIF-1 positive microglial cell body size was manually drawn using the Image Pro Plus measurement function, and expressed in μm^2. The roundness index of each microglia cell was calculated as reported in [36] with the equation: Roundness = $4A/\pi M^2$, where A is the area and M is the length of the major axis of each microglia cell's soma. Approximately 120 microglia cells were analysed from each sample.

Number and neuronal tracing of doublecortin (DCX)-positive cells – DCX-positive cells were counted in the subgranular zone and in the granular layer of the dentate gyrus, and expressed as number of neurons/100 µm. Dendritic trees of newborn DCX-positive granule neurons (15–20 per animal) were traced using custom-designed software for dendritic reconstruction (Immagini Computer, Milan, Italy), interfaced with Image Pro Plus. The dendritic tree was traced live, at a final magnification of 500X. The program provides the total dendritic length once the reconstruction of the entire dendritic tree is finished.

Microglia cell isolation

Microglial cells were isolated following the protocol published in [37]. Briefly, wild-type (+/+) and *Cdkl5* KO (+/-) female mice were anesthetized with 2% isoflurane (in pure oxygen) and transcardial perfused with PBS. Brains were transferred to ice-cold phosphate buffered saline (PBS; without Ca2 + and Mg2', with $NaHCO_3$, 0.75 g/l, Hepes buffer 10 mM, pH 7.4), freed of meninges, minced in serum-free Dulbecco modified Eagle medium (DMEM) containing 0.25% trypsin (T9201; Sigma-Aldrich, St. Louis, MO, USA) and 0.02% EDTA, and incubated at 37°C for 60 min. Enzymatic digestion was blocked by adding DMEM supplemented with 10% heat-inactivated FBS. After centrifugation (2000 rpm at 4°C for 5 min) samples were incubated with a DNAse I solution (serum-free DMEM containing 40 ug/ml DNAse Type I, D5025; Sigma-Aldrich, St. Louis, MO, USA) for 15 min at 37°C. Samples were then centrifuged, transferred to ice-cold DMEM, and sieved through a nylon mesh 40 µm pore size (Corning Cell Strainer). DMEM (21.4 ml) with sieved tissue derived from 2 mice brain was mixed with 8.6 ml of cold isotonic Percoll (Formerly GE Healthcare Life Sciences; Fisher scientific) in PBS and centrifuged (2000 rpm at 4°C for 20 min). Pellet was washed in PBS and finally resuspended in 1 ml of TRI reagent (Sigma-Aldrich, St. Louis, MO, USA) and stored at -80°C or processed for RNA extraction.

RNA isolation and RT-qPCR

Microglia cell RNA isolation was performed using the Direct-zol RNA MiniPrep kit (Zymo Research) and cDNA synthesis was achieved with 1 µg of total RNA using iScript™ Advanced cDNA Synthesis Kit (Bio-Rad, Hercules, CA, USA) according to the manufacturer's instructions. Real-time PCR was performed using Sso Advanced Universal SYBR Green Supermix (Bio-Rad) in an iQ5 Real-Time PCR Detection System (Bio-Rad). We used primer pairs (table S1) that gave an efficiency close to 100%. GAPDH (glyceraldehyde 3-phosphate dehydrogenase) used as a reference gene for normalization in the qPCR. Relative quantification was performed using the ΔΔCt method.

Western blotting

For the preparation of total cell extracts, tissue samples were homogenized in RIPA buffer (50 mMTris–HCl, pH 7.4, 150 mM NaCl, 1% Triton-X100, 0.5% sodium deoxycholate, 0.1% SDS) supplemented with 1 mM PMSF and 1% protease and phosphatase inhibitor cocktail (Sigma-Aldrich). Protein concentration was determined using the Bradford method [38]. Equivalent amounts (50 µg) of protein were subjected to electrophoresis on a 4–12% Mini-PROTEAN® TGX™ Gel (Bio-Rad) and transferred to a Hybond ECL nitrocellulose membrane (GE Healthcare Bio-Science). The following primary antibodies were used: rabbit polyclonal anti-GAPDH (1:5000, Sigma-Aldrich), rabbit polyclonal anti-STAT3 (1:1000, Sigma-Aldrich), rabbit polyclonal anti-phospho-STAT3 (1:1000, Cell Signaling Technology), and rabbit polyclonal anti-BDNF (1:500, Santa Cruz Biotechnology). An HRP-conjugated goat anti-rabbit IgG (1:5000, Jackson ImmunoResearch Laboratories) secondary antibody was used. Densitometric analysis of digitized images was performed using Chemidoc XRS Imaging Systems and Image LabTM Software (Bio-Rad).

Statistical analysis

Statistical analysis was performed with GraphPad Prism (version 7). Values are expressed as means ± standard error (SEM). The significance of results was obtained using Two-tailed unpaired t-test and one-way or two-way ANOVA followed by Fisher's LSD post-hoc test as specified in the figure legends. A probability level of $P < 0.05$ was considered to be statistically significant. The confidence level was taken as 95%.

Results

Increased microglial activation in the brain of Cdkl5 KO mice.

To investigate whether inflammatory processes could be involved in the pathophysiology of CDD, we counted the number and analyzed the morphology of microglia (AIF-1-positive cells) in the hippocampus and cortex of male (-/Y) and female (+/-) *Cdkl5* KO mice and wild-type (+/Y, +/+) littermates. We found an increase in the number of microglial cells in both the analyzed brain regions of -/Y and +/- *Cdkl5* KO mice in comparison with their +/Y, and +/+ counterparts (Fig. 1A-C). Moreover, microglial cells in *Cdkl5* KO mice presented an enlarged body size (Fig. 1D and Fig S1A,B) and reduced roundness of the cell body (Fig. 1E) compared to wild-type counterparts (Fig. 1B,D,E). Together, these data indicate that in the absence of *Cdkl5* microglia adopted a bigger, more irregular soma shape, typical of a state of activation [39].

Importantly, replacement of CDKL5 protein through a systemic injection of a TATκ-GFP-CDKL5 fusion protein [34] reversed microglial activation in Cdkl5 KO mice. We found a lower number of microglial cells (Fig. 2A) with a smaller body size (Fig. 2B) in the hippocampus and cortex of TATκ-GFP-CDKL5-treated *Cdkl5* -/Y mice compared to *Cdkl5* -/Y mice treated with a TATκ-GFP control protein, indicating the reversibility of the inflammatory phenotype due to the absence of Cdkl5.

Non-cell autonomous microglial activation in the absence of Cdkl5

In order to investigate whether microglial activation in *Cdkl5* KO mice is a cell-autonomous effect, we first evaluated Cdkl5 expression levels in purified microglial cells. Real time and western blot analyses showed

very low mRNA levels (Fig. 3A) and undetectable protein levels (Fig. 3B) of Cdkl5 in microglial cells compared to cortical extracts of wild-type mice, suggesting that Cdkl5 function is of minor relevance in these cells. Next, we evaluated the microglia activation status in *Emx1* KO mice, a conditional *Cdkl5* KO mouse model carrying *Cdkl5* deletion only in the excitatory neurons of the forebrain, but not in microglial cells [6, 35]. Similarly to *Cdkl5* KO mice, activation of microglial cells, increased number and body size of microglial cells (Fig. 3C), was present in the hippocampus of *Emx1* KO mice, suggesting a non-cell autonomous microglial over-activation in the absence of Cdkl5.

Treatment with luteolin inhibits microglia over-activation in Cdkl5 +/- mice.

Luteolin, a naturally occurring polyphenolic flavonoid, is a potent microglia inhibitor that possesses antioxidant, anti-inflammatory, and neuroprotective effects both *in vitro* and *in vivo* [40, 41]. Since the majority of CDD patients are heterozygous females [42], we tested the efficacy of an *in vivo* treatment with luteolin on microglial over-activation in the heterozygous female mouse model of CDD (+/-). Three-month-old *Cdkl5* KO female mice (+/-) were injected daily with luteolin (i.p. 10 mg/Kg) for 7 or 20 days. While both short and long term treatments with luteolin did not affect microglia cell number in the cortex of *Cdkl5* +/- mice (Fig. 4A,C), a 7-day treatment was sufficient to recover microglia body size at the wild-type level in both cortex (Fig. 4B,C) and hippocampus (Fig. S2).

Confirming microglia over-activation, we found significantly higher levels of phosphorylated STAT3, a key promoter of microglial cell pro-inflammatory phenotype [43, 44], in brain homogenates of *Cdkl5* +/- mice in comparison with their wild-type counterparts (Fig. 4D-F). A 7-day treatment with luteolin restored phospho-STAT3 levels to those of wild-type mice (Fig. 4D,F). No differences in total STAT3 levels were observed in treated or untreated *Cdkl5* +/- mice in comparison with their wild-type counterparts (Fig. 4E,F).

Accordingly with activation of STAT3 signaling and microglia over-activation, we found increased expression of molecules involved in the microglial neuroinflammatory response, such as IL-1β and IL-6 cytokines, and TNFα or microglial markers (CX3CR1 and AIF-1) (Fig. 5A,B); the increased expression was recovered by treatment with luteolin in *Cdkl5* +/- mice (Fig. 5A,B).

Treatment with luteolin restores survival and maturation of newborn cells in the dentate gyrus of Cdkl5 +/- mice

Loss of Cdkl5 impairs survival and maturation of newborn hippocampal neurons [11, 16]. In order to evaluate the efficacy of *in vivo* treatment with luteolin on the survival rate of new neurons, we assessed the number of doublecortin (DCX)-positive cells in the dentate gyrus (DG) of untreated *Cdkl5* +/- and *Cdkl5* +/+ mice and *Cdkl5* +/- mice treated with luteolin for 7 days. We found that treatment with luteolin restored the number of DCX-positive granule neurons in *Cdkl5* +/- mice (Fig. 6A,B). To determine whether increased proliferation rate underlies the positive effect of luteolin on newborn neuronal number, we counted proliferating cells immunostained for Ki-67, an endogenous marker of actively proliferating cells. We found that luteolin-treated *Cdkl5* +/– mice had the same number of Ki-67 labelled cells as untreated

Cdkl5 +/− and *Cdkl5* +/+ mice (Fig. 6C). This evidence indicates that the higher number of DCX-positive cells in treated *Cdkl5* +/− mice is not due to an increase in proliferation rate.

Importantly, luteolin treatment improved impaired dendritic development in *Cdkl5* +/- mice. Quantification of the dendritic tree of DCX positive cells showed that *Cdkl5* +/− mice had a shorter dendritic length than wild-type mice (Fig. 6A,D); a 7-day treatment with luteolin improved this defect (Fig. 6A,D).

It was reported that luteolin treatment increases brain levels of the brain-derived neurotrophic factor (BDNF) [33], which is necessary for neuronal survival and maturation [45]. We examined mature BDNF levels in cortical homogenates of *Cdkl5* +/- and *Cdkl5* +/+ mice and in *Cdkl5* +/- mice following administration of luteolin for 7 days. While levels of BDNF were similar in *Cdkl5* +/- and *Cdkl5* +/+ mice treated with the vehicle, treatment with luteolin increased levels of BDNF by about 50% (Fig. 6E,F).

Microglia activation with age in Cdkl5 +/- mice

To assess whether microglia over-activation is already present at an early stage of life and to monitor its evolution with age, we analyzed microglial cell status in the brains of *Cdkl5* KO mice at different developmental stages (young: 20-day-old, adult: 3-month-old, and middle-aged: 11-month-old mice). We found that an increase in microglial cell number and soma size was already present in the cortex and hippocampus of young *Cdkl5* +/- mice compared to their wild-type counterparts of the same age (Fig. 7A,B). A significant decrease in the density of microglial cells with age was present in both wild-type and *Cdkl5* +/- mice compared to their 20-day-old counterparts (Fig. 7A,B). Surprisingly, while the difference in the number of microglial cells was maintained between *Cdkl5* +/- and wild-type mice at 3 months of age, in middle-aged mice there was no longer a difference (Fig. 7A,B). In contrast, increased microglial body size in *Cdkl5* +/- mice was present in all three age groups compared to their wild-type counterparts of the same age (Fig. 7A,B). Interestingly, an age-dependent worsening of microglial activation, and, therefore, microglial body size, was observed in both middle-aged *Cdkl5* +/- and *Cdkl5* +/+ mice (Fig. 7A,B).

Luteolin treatment restores neuron survival in middle-aged Cdkl5 +/- mice

Microglial cell changes compatible with their activation have been documented in aging [46, 47] and it has been suggested that they contribute to the brain decline in pathological conditions [48, 49]. Recent evidence showed an age-dependent decreased hippocampal neuron survival in middle-aged *Cdkl5* KO mice, paralleled by an increased cognitive decline [21].

To explore the possibility that microglia over-activation in aged *Cdkl5* KO mice could underlie the higher neuronal loss, we assessed the efficacy of treatment with luteolin in counteracting neuronal loss in 11-month-old *Cdkl5* +/- mice (Fig. 8A). Treatment with luteolin reduced microglia body size in the hippocampus of middle-aged *Cdkl5* +/- mice at even lower levels than those of wild-type mice of the same age (Fig. 8B). Importantly, the reduced number of Hoechst-positive nuclei (Fig. 8C) and NeuN-

positive cells (Fig. 8D) in middle-aged *Cdkl5* +/- mice was strongly improved by treatment with luteolin (Fig. 8C,D).

Treatment with luteolin prevents NMDA-induced excitotoxicity in the hippocampus of Cdkl5 +/- mice.

To investigate whether microglia over-activation has a causative role in the increased neuronal susceptibility to excitotoxic stress in *Cdkl5* KO mice [19, 20], we pre-treated *Cdkl5* +/- mice for 7 days with Luteolin before NMDA (60mg/kg) intraperitoneal injection (Fig. 9A). Animals were sacrificed 1 day or 8 days after NMDA administration (Fig. 9A). As expected, microglia activation increased in the hippocampus of both *Cdkl5* +/- and *Cdkl5* +/+ mice after NMDA treatment (Fig. 9B). Nevertheless, after NMDA excitotoxic stimulation, the somal volume of microglial cells in *Cdkl5* +/- mice was higher than that of NMDA-treated wild-type mice (Fig. 9B). Importantly, luteolin treatment was able to counteract both basal and NMDA-induced microglial activation in *Cdkl5* KO mice, bringing microglial soma size back to that of the untreated wild-type mouse condition (Fig. 9B).

Neuronal death was assessed 1 day after NMDA administration using immunohistochemistry for cleaved caspase-3 and 8 days after using Hoechst staining and immunohistochemistry for NeuN. In the CA1 layer of the hippocampus, NMDA-treated *Cdkl5* +/- mice showed a higher number of cleaved caspase-3 positive cells (Fig. 9C,D) and a lower number of Hoechst-positive nuclei (Fig. 9E) and NeuN-positive cells (Fig. 9F,G) in comparison with NMDA-treated wild-type mice, indicating increased cell death in *Cdkl5* +/- mice after the excitotoxic stimulus. Importantly, pre-treatment with luteolin reduced cell death at 24 h after NMDA treatment in *Cdkl5* +/- mice (Fig. 9C,D), thus preventing neuronal loss in the hippocampal CA1 region (Fig. 9E-G).

Discussion

The lack of effective therapies for CDD stresses the urgency with which pathogenic mechanisms underlying the disorder need to be identified. Our results highlight, for the first time, the presence of a generalized status of microglia over-activation in the brain of a mouse model of CDD. We found alterations in microglial cell morphology and number, increased levels of AIF-1 and proinflammatory cytokines, and increased STAT3 signaling in the brain of *Cdkl5* KO mice. Remarkably, treatment with luteolin (a natural anti-inflammatory flavonoid) is able to recover impaired neuronal survival and maturation in *Cdkl5* KO mice, suggesting that a hyperactive state of microglia plays a causative role in the CDD phenotype.

Recently, a cytokine dysregulation, proportional to clinical severity and redox imbalance, was found in children affected by CDD [31, 32]. Results included increased Tumour Necrosis Factor (TNF)-α, Interleukin (IL)-1β, and Interleukin (IL)-6 in the peripheral blood of children with CDD. These inflammatory cytokines could signal inflammatory changes in the brain that could, in turn, greatly impact neurodevelopment and neural function in CDD. Our finding of an over-activation of microglial cells with increased TNF-α, IL-1β and IL-6 levels in the brain of *Cdkl5* KO mice is in line with the results observed in CDD patients, and suggests the involvement of neuro-inflammatory processes in the pathophysiology of CDD.

Microglia activation, associated with an increase in cell body size, as well as cytokine alterations in the peripheral blood, has been recently described in neurodevelopmental disorders such as autism spectrum disorders (ASDs), Down syndrome, and Rett syndrome [28–30, 50, 51]. Similarly to Rett syndrome [52], the mechanism by which absence of *Cdkl5* induces microglia over-activation appeared to be non-cell autonomous. By using *Emx1* KO mice, a conditional *Cdkl5* KO mouse model which does not carry *Cdkl5* deletion in microglial cells [6, 35], we found that microglia over-activation is independent of microglia-specific loss of Cdkl5 expression. This finding suggests that microglial activation in the *Cdkl5* KO brain may be attributable to neuronal loss of Cdkl5. Accumulating evidence indicates the presence of bidirectional microglia-neuron communication in the healthy and diseased brain [53]. In the healthy brain, microglia exhibit an actively repressed 'surveying' phenotype that is dependent on a dynamic crosstalk between microglia and neurons [54]. It has been proposed that the removal of this neuronal-derived inhibitory control represents a type of danger signal for microglia, indicating that neuronal function is impaired and leads to alterations in microglia morphology and function. The chronic activation of microglia may, in turn, cause reduced neuronal maturation and survival through the release of potentially cytotoxic molecules such as proinflammatory cytokines [23, 24]. Our finding that inhibition of microglia over-activation by luteolin restores survival and maturation of newborn neurons in the hippocampal dentate gyrus of *Cdkl5* KO mice is in line with this hypothesis. Though luteolin treatment had no effect on the number of microglial cells, it restored microglia body size and shape, and, importantly, pro-inflammatory cytokines and P-STAT3 levels. Differently from a recent study that demonstrated the effect of luteolin treatment in increasing cell proliferation in a mouse model of Down syndrome [33], we did not observe an increased number of Ki-67-positive cells in the hippocampal dentate gyrus of *Cdkl5* KO mice. This discrepancy can be explained by a selective effect of luteolin on the Ts65Dn mouse, as the authors themselves did not observe a luteolin-dependent proliferation increase in wild-type mice. The pro-survival effect of microglial inhibition was confirmed by the restoration of the age-dependent decreased hippocampal neuron survival in middle-aged *Cdkl5* KO mice. This is in agreement with recent studies that suggest that luteolin plays a role in counteracting age-induced microglia activation in aged mice [55, 56].

The neuroprotective effect of luteolin might also be associated with its effect on increasing BDNF levels. Recent findings reported that luteolin increases the expression of BDNF in the cerebral cortex and hippocampus of mice [33, 57]. Similarly to these findings, we found increased BDNF levels in the brain of luteolin treated *Cdkl5* KO mice. Since BDNF plays an important role in the survival and development of neurons [58], it is reasonable to hypothesize that, in Cdkl5 KO mice, the luteolin-dependent activation of the BDNF pathways contributes to hippocampal neuronal survival and maturation.

As previously reported in male *Cdkl5* KO mice [19, 20], we found here that hippocampal neurons of heterozygous female *Cdkl5* KO mice showed an increased vulnerability to excitotoxicity. Inflammatory processes, including activation of microglia and production of proinflammatory cytokines, such as TNF-α, IL-1β, and IL-6, are associated with excitotoxic stimuli [59, 60]. Similarly, we observed an increased microglial over-activation in response to NMDA treatment. Importantly, the microglia activation was higher in *Cdkl5* KO mice than in wild-type mice. Luteolin pre-treatment recovered the increased NMDA-induced cell death in hippocampal neurons of *Cdkl5* KO mice. Because the increased cell death of

hippocampal neurons observed in response to NMDA treatment correlates with an increased microglial over-activation, the beneficial effect of luteolin in neuronal survival can be, at least partially, ascribed to the inhibition of microglia activation. Luteolin was observed to exert a similar neuroprotective activity against kainic acid-induced brain damage in mice [61].

Conclusions

Microglia remain to be controversial cells within the CNS, with both beneficial and detrimental roles, especially in the context of disease pathology. Our finding that treatment with luteolin recovers neuronal survival and maturation in *Cdkl5* KO mice supports the theory that microglia exert a harmful action in the CDKL5-null brain. Recent evidence strongly supports the role of neuroinflammation in the pathophysiology of human epilepsy [62]. In support of this it has been shown that pre-treatment with luteolin significantly reduces the frequency of drug-induced seizures in animal models of epilepsy [61, 63–65]. Since epilepsy is one of the hallmark features of CDD, it may be hypothesized that luteolin has a beneficial effect on this feature. Therefore, the suppression of microglia-mediated inflammation may be considered as an important strategy in CDD therapy.

Abbreviations

AIF-1 = Allograft inflammatory factor 1; ASD = Autism spectrum disorders; BDNF = brain-derived neurotrophic factor; CDD = CDKL5 Deficiency Disorder; DCX = Doublecortin; DG = dentate gyrus; IL-1β = Interleukin-1β; IL-6 = Interleukin-6; NMDA = N-Methyl-D-aspartate; PSD-95 = Postsynaptic density protein 95; STAT3 = Signal transducer and activator of transcription 3; TNF-α = Tumor necrosis factor-α.

Declarations

Ethics approval and consent to participate

All research and animal care procedures were performed according to protocols approved by the Italian Ministry for Health and by the Bologna University Bioethical Committee.

Consent for publication

Not applicable.

Availability of data and materials

The datasets analyzed during the current study are available from the corresponding author on reasonable request.

Competing interests

The authors declare that they have no competing interests.

Funding

This work was supported by the Telethon foundation (grant number GGP19045 to EC), and by the Italian parent associations “CDKL5 insieme verso la cura” to EC.

Authors' contributions

GG, NM and LG performed the experiments. ML and GM analyzed the data. MT and CF helped in the experiment. EC and ST designed the experiments and wrote the manuscript. All authors read and approved the final manuscript.

Acknowledgements

Not applicable.

References

1. Montini E, Andolfi G, Caruso A, Buchner G, Walpole SM, Mariani M, Consalez G, Trump D, Ballabio A, Franco B: Identification and characterization of a novel serine-threonine kinase gene from the Xp22 region. Genomics 1998, 51:427-433.
2. Rusconi L, Salvatoni L, Giudici L, Bertani I, Kilstrup-Nielsen C, Broccoli V, Landsberger N: CDKL5 expression is modulated during neuronal development and its subcellular distribution is tightly regulated by the C-terminal tail. J Biol Chem 2008, 283:30101-30111.
3. Demarest S, Pestana-Knight EM, Olson HE, Downs J, Marsh ED, Kaufmann WE, Partridge CA, Leonard H, Gwadry-Sridhar F, Frame KE, et al: Severity Assessment in CDKL5 Deficiency Disorder. Pediatr Neurol 2019, 97:38-42.
4. Fehr S, Wilson M, Downs J, Williams S, Murgia A, Sartori S, Vecchi M, Ho G, Polli R, Psoni S, et al: The CDKL5 disorder is an independent clinical entity associated with early-onset encephalopathy. Eur J Hum Genet 2013, 21:266-273.
5. Mangatt M, Wong K, Anderson B, Epstein A, Hodgetts S, Leonard H, Downs J: Prevalence and onset of comorbidities in the CDKL5 disorder differ from Rett syndrome. Orphanet J Rare Dis 2016, 11:39.
6. Amendola E, Zhan Y, Mattucci C, Castroflorio E, Calcagno E, Fuchs C, Lonetti G, Silingardi D, Vyssotski AL, Farley D, et al: Mapping pathological phenotypes in a mouse model of CDKL5 disorder. PLoS One 2014, 9:e91613.
7. Tang S, Wang IJ, Yue C, Takano H, Terzic B, Pance K, Lee JY, Cui Y, Coulter DA, Zhou Z: Loss of CDKL5 in Glutamatergic Neurons Disrupts Hippocampal Microcircuitry and Leads to Memory Impairment in Mice. J Neurosci 2017, 37:7420-7437.
8. Wang IT, Allen M, Goffin D, Zhu X, Fairless AH, Brodkin ES, Siegel SJ, Marsh ED, Blendy JA, Zhou Z: Loss of CDKL5 disrupts kinome profile and event-related potentials leading to autistic-like phenotypes in mice. Proc Natl Acad Sci U S A 2012, 109:21516-21521.

9. Okuda K, Takao K, Watanabe A, Miyakawa T, Mizuguchi M, Tanaka T: Comprehensive behavioral analysis of the Cdkl5 knockout mice revealed significant enhancement in anxiety- and fear-related behaviors and impairment in both acquisition and long-term retention of spatial reference memory. PLoS One 2018, 13:e0196587.
10. Fuchs C, Gennaccaro L, Trazzi S, Bastianini S, Bettini S, Lo Martire V, Ren E, Medici G, Zoccoli G, Rimondini R, Ciani E: Heterozygous CDKL5 Knockout Female Mice Are a Valuable Animal Model for CDKL5 Disorder. Neural Plast 2018, 2018:9726950.
11. Fuchs C, Trazzi S, Torricella R, Viggiano R, De Franceschi M, Amendola E, Gross C, Calza L, Bartesaghi R, Ciani E: Loss of CDKL5 impairs survival and dendritic growth of newborn neurons by altering AKT/GSK-3beta signaling. Neurobiol Dis 2014, 70:53-68.
12. Lo Martire V, Alvente S, Bastianini S, Berteotti C, Silvani A, Valli A, Viggiano R, Ciani E, Zoccoli G: CDKL5 deficiency entails sleep apneas in mice. J Sleep Res 2017, 26:495-497.
13. Mazziotti R, Lupori L, Sagona G, Gennaro M, Della Sala G, Putignano E, Pizzorusso T: Searching for biomarkers of CDKL5 disorder: early-onset visual impairment in CDKL5 mutant mice. Hum Mol Genet 2017, 26:2290-2298.
14. Jhang CL, Lee HY, Chen JC, Liao W: Dopaminergic loss of cyclin-dependent kinase-like 5 recapitulates methylphenidate-remediable hyperlocomotion in mouse model of CDKL5 deficiency disorder. Hum Mol Genet 2020, 29:2408-2419.
15. Fuchs C, Rimondini R, Viggiano R, Trazzi S, De Franceschi M, Bartesaghi R, Ciani E: Inhibition of GSK3beta rescues hippocampal development and learning in a mouse model of CDKL5 disorder. Neurobiol Dis 2015, 82:298-310.
16. Trazzi S, Fuchs C, Viggiano R, De Franceschi M, Valli E, Jedynak P, Hansen FK, Perini G, Rimondini R, Kurz T, et al: HDAC4: a key factor underlying brain developmental alterations in CDKL5 disorder. Hum Mol Genet 2016, 25:3887-3907.
17. Della Sala G, Putignano E, Chelini G, Melani R, Calcagno E, Michele Ratto G, Amendola E, Gross CT, Giustetto M, Pizzorusso T: Dendritic Spine Instability in a Mouse Model of CDKL5 Disorder Is Rescued by Insulin-like Growth Factor 1. Biol Psychiatry 2016, 80:302-311.
18. Pizzo R, Gurgone A, Castroflorio E, Amendola E, Gross C, Sassoe-Pognetto M, Giustetto M: Lack of Cdkl5 Disrupts the Organization of Excitatory and Inhibitory Synapses and Parvalbumin Interneurons in the Primary Visual Cortex. Front Cell Neurosci 2016, 10:261.
19. Loi M, Trazzi S, Fuchs C, Galvani G, Medici G, Gennaccaro L, Tassinari M, Ciani E: Increased DNA Damage and Apoptosis in CDKL5-Deficient Neurons. Mol Neurobiol 2020, 57:2244-2262.
20. Fuchs C, Medici G, Trazzi S, Gennaccaro L, Galvani G, Berteotti C, Ren E, Loi M, Ciani E: CDKL5 deficiency predisposes neurons to cell death through the deregulation of SMAD3 signaling. Brain Pathol 2019, 29:658-674.
21. Gennaccaro L, Fuchs C, Loi M, Pizzo R, Alvente S, Berteotti C, Lupori L, Sagona G, Galvani G, Gurgone A, et al: Age-Related Cognitive and Motor Decline in a Mouse Model of CDKL5 Deficiency Disorder is Associated with Increased Neuronal Senescence and Death. Aging and disease 2021.

22. Ginhoux F, Lim S, Hoeffel G, Low D, Huber T: Origin and differentiation of microglia. Front Cell Neurosci 2013, 7:45.
23. Lull ME, Block ML: Microglial activation and chronic neurodegeneration. Neurotherapeutics 2010, 7:354-365.
24. Wang WY, Tan MS, Yu JT, Tan L: Role of pro-inflammatory cytokines released from microglia in Alzheimer's disease. Ann Transl Med 2015, 3:136.
25. Bartels T, De Schepper S, Hong S: Microglia modulate neurodegeneration in Alzheimer's and Parkinson's diseases. Science 2020, 370:66-69.
26. Gray SC, Kinghorn KJ, Woodling NS: Shifting equilibriums in Alzheimer's disease: the complex roles of microglia in neuroinflammation, neuronal survival and neurogenesis. Neural Regen Res 2020, 15:1208-1219.
27. Sabogal-Guaqueta AM, Marmolejo-Garza A, de Padua VP, Eggen B, Boddeke E, Dolga AM: Microglia alterations in neurodegenerative diseases and their modeling with human induced pluripotent stem cell and other platforms. Prog Neurobiol 2020, 190:101805.
28. Pinto B, Morelli G, Rastogi M, Savardi A, Fumagalli A, Petretto A, Bartolucci M, Varea E, Catelani T, Contestabile A, et al: Rescuing Over-activated Microglia Restores Cognitive Performance in Juvenile Animals of the Dp(16) Mouse Model of Down Syndrome. Neuron 2020, 108:887-904 e812.
29. Matta SM, Hill-Yardin EL, Crack PJ: The influence of neuroinflammation in Autism Spectrum Disorder. Brain Behav Immun 2019, 79:75-90.
30. Jin XR, Chen XS, Xiao L: MeCP2 Deficiency in Neuroglia: New Progress in the Pathogenesis of Rett Syndrome. Front Mol Neurosci 2017, 10:316.
31. Leoncini S, De Felice C, Signorini C, Zollo G, Cortelazzo A, Durand T, Galano JM, Guerranti R, Rossi M, Ciccoli L, Hayek J: Cytokine Dysregulation in MECP2- and CDKL5-Related Rett Syndrome: Relationships with Aberrant Redox Homeostasis, Inflammation, and omega-3 PUFAs. Oxid Med Cell Longev 2015, 2015:421624.
32. Cortelazzo A, de Felice C, Leoncini S, Signorini C, Guerranti R, Leoncini R, Armini A, Bini L, Ciccoli L, Hayek J: Inflammatory protein response in CDKL5-Rett syndrome: evidence of a subclinical smouldering inflammation. Inflamm Res 2017, 66:269-280.
33. Zhou WB, Miao ZN, Zhang B, Long W, Zheng FX, Kong J, Yu B: Luteolin induces hippocampal neurogenesis in the Ts65Dn mouse model of Down syndrome. Neural Regen Res 2019, 14:613-620.
34. Trazzi S, De Franceschi M, Fuchs C, Bastianini S, Viggiano R, Lupori L, Mazziotti R, Medici G, Lo Martire V, Ren E, et al: CDKL5 protein substitution therapy rescues neurological phenotypes of a mouse model of CDKL5 disorder. Hum Mol Genet 2018, 27:1572-1592.
35. Lupori L, Sagona G, Fuchs C, Mazziotti R, Stefanov A, Putignano E, Napoli D, Strettoi E, Ciani E, Pizzorusso T: Site-specific abnormalities in the visual system of a mouse model of CDKL5 deficiency disorder. Hum Mol Genet 2019, 28:2851-2861.
36. Davis BM, Salinas-Navarro M, Cordeiro MF, Moons L, De Groef L: Characterizing microglia activation: a spatial statistics approach to maximize information extraction. Sci Rep 2017, 7:1576.

37. Slepko N, Levi G: Progressive activation of adult microglial cells in vitro. Glia 1996, 16:241-246.
38. Bradford MM: A rapid and sensitive method for the quantitation of microgram quantities of protein utilizing the principle of protein-dye binding. Anal Biochem 1976, 72:248-254.
39. Torres-Platas SG, Comeau S, Rachalski A, Bo GD, Cruceanu C, Turecki G, Giros B, Mechawar N: Morphometric characterization of microglial phenotypes in human cerebral cortex. J Neuroinflammation 2014, 11:12.
40. Ashaari Z, Hadjzadeh MA, Hassanzadeh G, Alizamir T, Yousefi B, Keshavarzi Z, Mokhtari T: The Flavone Luteolin Improves Central Nervous System Disorders by Different Mechanisms: A Review. J Mol Neurosci 2018, 65:491-506.
41. Aziz N, Kim MY, Cho JY: Anti-inflammatory effects of luteolin: A review of in vitro, in vivo, and in silico studies. J Ethnopharmacol 2018, 225:342-358.
42. Bahi-Buisson N, Bienvenu T: CDKL5-Related Disorders: From Clinical Description to Molecular Genetics. Mol Syndromol 2012, 2:137-152.
43. Przanowski P, Dabrowski M, Ellert-Miklaszewska A, Kloss M, Mieczkowski J, Kaza B, Ronowicz A, Hu F, Piotrowski A, Kettenmann H, et al: The signal transducers Stat1 and Stat3 and their novel target Jmjd3 drive the expression of inflammatory genes in microglia. J Mol Med (Berl) 2014, 92:239-254.
44. Jin X, Liu MY, Zhang DF, Zhong X, Du K, Qian P, Gao H, Wei MJ: Natural products as a potential modulator of microglial polarization in neurodegenerative diseases. Pharmacol Res 2019, 145:104253.
45. Kowianski P, Lietzau G, Czuba E, Waskow M, Steliga A, Morys J: BDNF: A Key Factor with Multipotent Impact on Brain Signaling and Synaptic Plasticity. Cell Mol Neurobiol 2018, 38:579-593.
46. Sheng JG, Mrak RE, Griffin WS: Enlarged and phagocytic, but not primed, interleukin-1 alpha-immunoreactive microglia increase with age in normal human brain. Acta Neuropathol 1998, 95:229-234.
47. Miller KR, Streit WJ: The effects of aging, injury and disease on microglial function: a case for cellular senescence. Neuron Glia Biol 2007, 3:245-253.
48. Spittau B: Aging Microglia-Phenotypes, Functions and Implications for Age-Related Neurodegenerative Diseases. Front Aging Neurosci 2017, 9:194.
49. von Bernhardi R, Tichauer JE, Eugenin J: Aging-dependent changes of microglial cells and their relevance for neurodegenerative disorders. J Neurochem 2010, 112:1099-1114.
50. Martini AC, Helman AM, McCarty KL, Lott IT, Doran E, Schmitt FA, Head E: Distribution of microglial phenotypes as a function of age and Alzheimer's disease neuropathology in the brains of people with Down syndrome. Alzheimers Dement (Amst) 2020, 12:e12113.
51. Kahanovitch U, Patterson KC, Hernandez R, Olsen ML: Glial Dysfunction in MeCP2 Deficiency Models: Implications for Rett Syndrome. Int J Mol Sci 2019, 20.
52. Schafer DP, Heller CT, Gunner G, Heller M, Gordon C, Hammond T, Wolf Y, Jung S, Stevens B: Microglia contribute to circuit defects in Mecp2 null mice independent of microglia-specific loss of

Mecp2 expression. Elife 2016, 5.

53. Szepesi Z, Manouchehrian O, Bachiller S, Deierborg T: Bidirectional Microglia-Neuron Communication in Health and Disease. Front Cell Neurosci 2018, 12:323.
54. Biber K, Neumann H, Inoue K, Boddeke HW: Neuronal 'On' and 'Off' signals control microglia. Trends Neurosci 2007, 30:596-602.
55. Jang S, Dilger RN, Johnson RW: Luteolin inhibits microglia and alters hippocampal-dependent spatial working memory in aged mice. J Nutr 2010, 140:1892-1898.
56. Burton MD, Rytych JL, Amin R, Johnson RW: Dietary Luteolin Reduces Proinflammatory Microglia in the Brain of Senescent Mice. Rejuvenation Res 2016, 19:286-292.
57. Liu R, Gao M, Qiang GF, Zhang TT, Lan X, Ying J, Du GH: The anti-amnesic effects of luteolin against amyloid beta(25-35) peptide-induced toxicity in mice involve the protection of neurovascular unit. Neuroscience 2009, 162:1232-1243.
58. Lee S, Yang M, Kim J, Son Y, Kim J, Kang S, Ahn W, Kim SH, Kim JC, Shin T, et al: Involvement of BDNF/ERK signaling in spontaneous recovery from trimethyltin-induced hippocampal neurotoxicity in mice. Brain Res Bull 2016, 121:48-58.
59. Kim DH, Yoon BH, Jung WY, Kim JM, Park SJ, Park DH, Huh Y, Park C, Cheong JH, Lee KT, et al: Sinapic acid attenuates kainic acid-induced hippocampal neuronal damage in mice. Neuropharmacology 2010, 59:20-30.
60. Zhang XM, Jin T, Quezada HC, Mix E, Winblad B, Zhu J: Kainic acid-induced microglial activation is attenuated in aged interleukin-18 deficient mice. J Neuroinflammation 2010, 7:26.
61. Lin TY, Lu CW, Wang SJ: Luteolin protects the hippocampus against neuron impairments induced by kainic acid in rats. Neurotoxicology 2016, 55:48-57.
62. Aronica E, Bauer S, Bozzi Y, Caleo M, Dingledine R, Gorter JA, Henshall DC, Kaufer D, Koh S, Loscher W, et al: Neuroinflammatory targets and treatments for epilepsy validated in experimental models. Epilepsia 2017, 58 Suppl 3:27-38.
63. Birman H, Dar KA, Kapucu A, Acar S, Uzum G: Effects of Luteolin on Liver, Kidney and Brain in Pentylentetrazol-Induced Seizures: Involvement of Metalloproteinases and NOS Activities. Balkan Med J 2012, 29:188-196.
64. Zhen JL, Chang YN, Qu ZZ, Fu T, Liu JQ, Wang WP: Luteolin rescues pentylenetetrazole-induced cognitive impairment in epileptic rats by reducing oxidative stress and activating PKA/CREB/BDNF signaling. Epilepsy Behav 2016, 57:177-184.
65. Tambe R, Patil A, Jain P, Sancheti J, Somani G, Sathaye S: Assessment of luteolin isolated from Eclipta alba leaves in animal models of epilepsy. Pharm Biol 2017, 55:264-268.

Figures

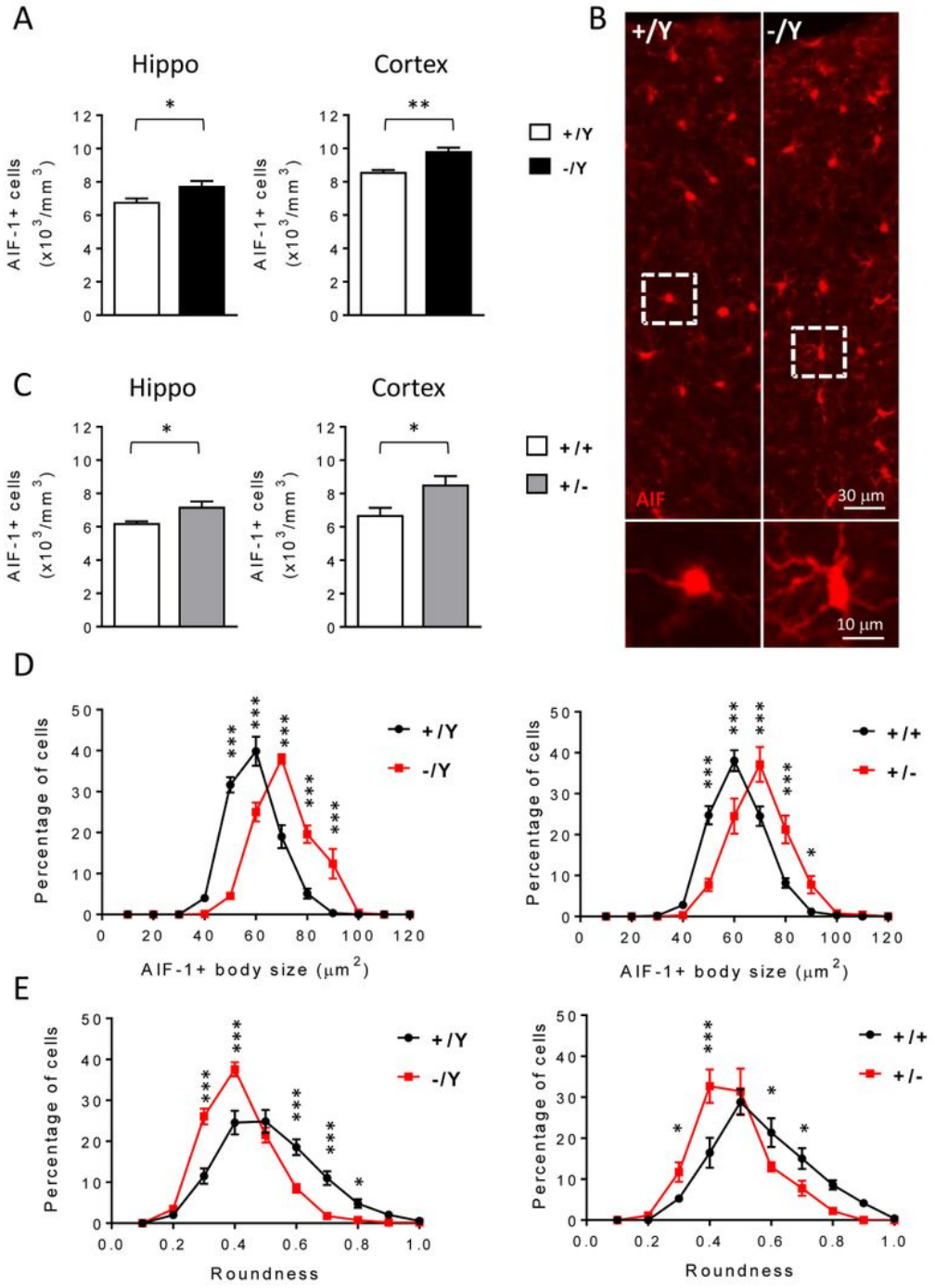

Figure 1

Increased microglial activation in the brain of Cdkl5 KO mice. A,C: Quantification of AIF-1-positive cells in hippocampal (Hippo) and somatosensory cortex (Cortex) sections from 3-month-old male (+/Y n=4, -/Y n=4; A), and female (+/+ n=5, +/- n=6; C) Cdkl5 KO mice. B: Representative fluorescence images of cortical sections processed for AIF-1 immunohistochemistry of a wild-type (+/Y) and a Cdkl5 KO mouse (-/Y). The dotted boxes in the upper panels indicate microglial cells shown in magnification in lower

panels. D: Distribution analysis of microglial cells soma area in the somatosensory cortex of 3-month-old male (+/Y n=4, -/Y n=4 on the left), and female (+/+ n=4, +/- n=6 on the right) Cdkl5 KO mice, showing a shift to larger cell body sizes in the absence of Cdkl5. E: Distribution analysis of microglial cell circularity (roundness) in the somatosensory cortex of Cdkl5 KO mice as in D. In Cdkl5 KO mice microglial cells are more irregularly shaped (lower roundness index) showing a left-shifted distribution compared to that of wild-type mice. The results in A and C are presented as means ± SEM. * p<0.05; ** p<0.01; ***p<0.001 (two-tailed Student's t-test). The results in D and E are presented as means ± SEM. * p<0.05; ***p<0.001 (Fisher's LSD test after two-way ANOVA).

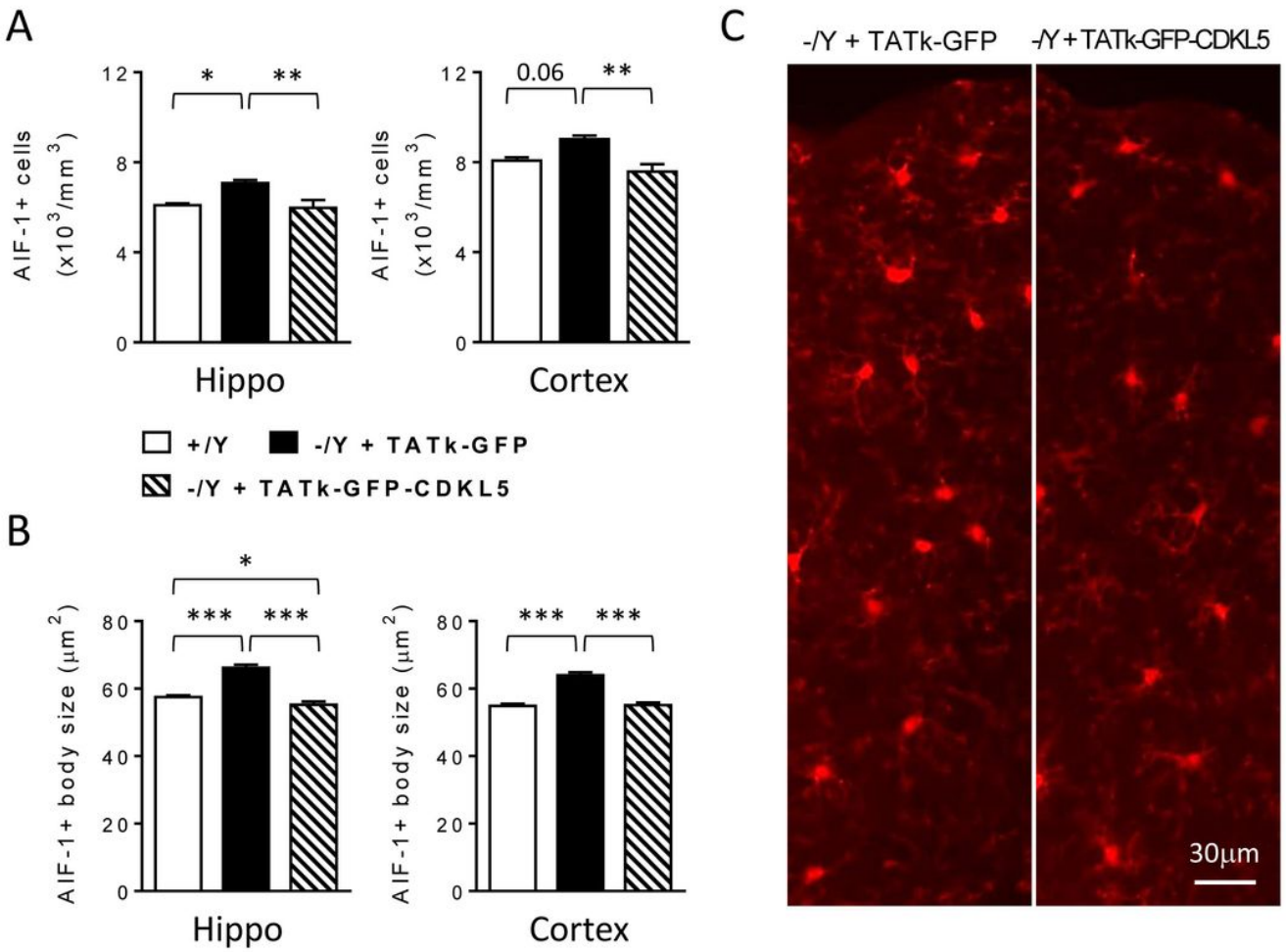

Figure 2

Effect of TATκ-GFP-CDKL5 administration on microglial cell activation in Cdkl5 KO mice. A: Quantification of AIF-1-positive cells in hippocampal (Hippo) and somatosensory cortex (Cortex) sections from 6-month-old wild-type (+/Y n=2) mice and Cdkl5 -/Y mice treated with TATκ-GFP (n= 5) or TATκ-GFP-CDKL5 (n= 5) protein as described in [34]. B: Mean microglia cell body size in the hippocampus and somatosensory cortex of Cdkl5 KO mice as in A. Data in A and B are presented as means ± SEM. * p<0.05; ** p<0.01; ***p<0.001 (Fisher's LSD after one-way ANOVA). C: Examples of cortical sections

processed for AIF-1 immunostaining of a Cdkl5 -/Y mouse treated with TATκ-GFP or TATκ-GFP-CDKL5 as in A.

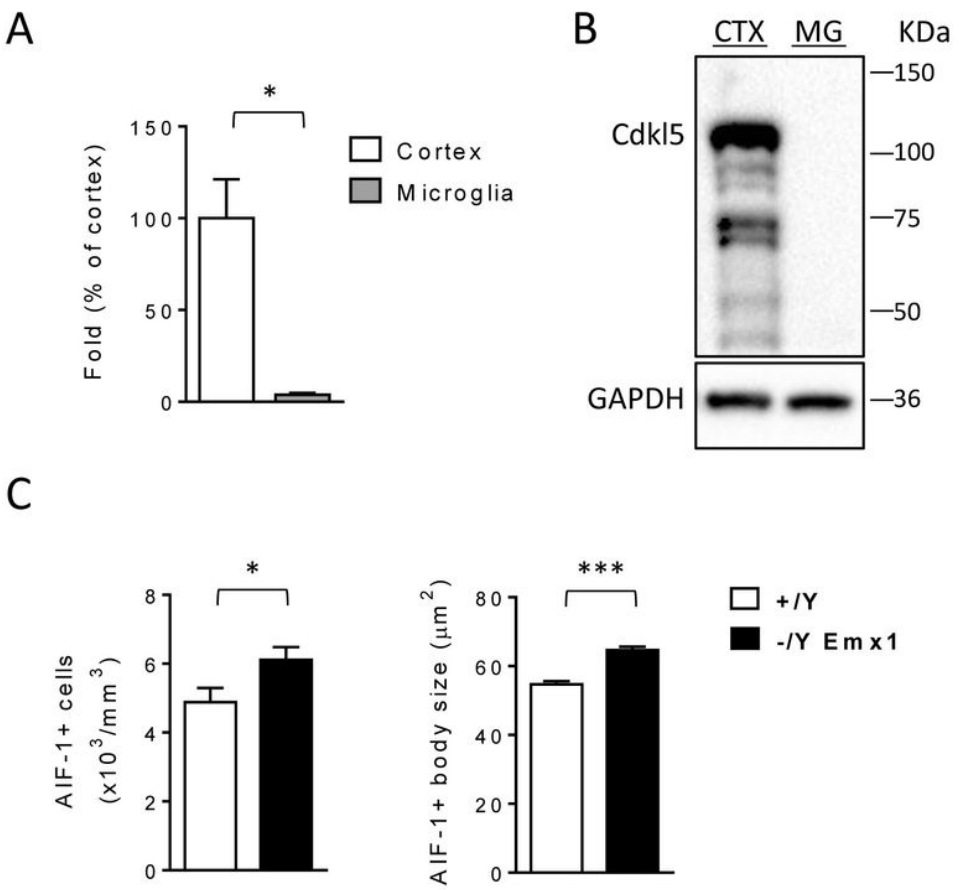

Figure 3

Non-cell autonomous microglial activation in the absence of Cdkl5. A: Expression of Cdkl5 mRNA in cortex of 3-month-old Cdkl5 +/+ mice (n=3) and microglial cells purified from 3-month-old Cdkl5 +/+ mice (n=3). Data are given as a percentage of Cdkl5 cortical expression. B: Example of immunoblot showing Cdkl5 and GAPDH levels in extracts from somatosensory cortex (CTX) of a wild-type Cdkl5 +/+ mouse and from microglial cells (MG) purified from Cdkl5 +/+ mice (n=4). C: Quantification of AIF-1-positive cells (on the left) and mean cell body size (on the right) of microglial cells in hippocampal sections of wild-type (+/Y; n=4) and Emx1 KO (-/Y Emx1; n=5) mice. The results in A and C are presented as means ± SEM. * p<0.05; **P< 0.01; ***p<0.001 (two-tailed Student's t-test).

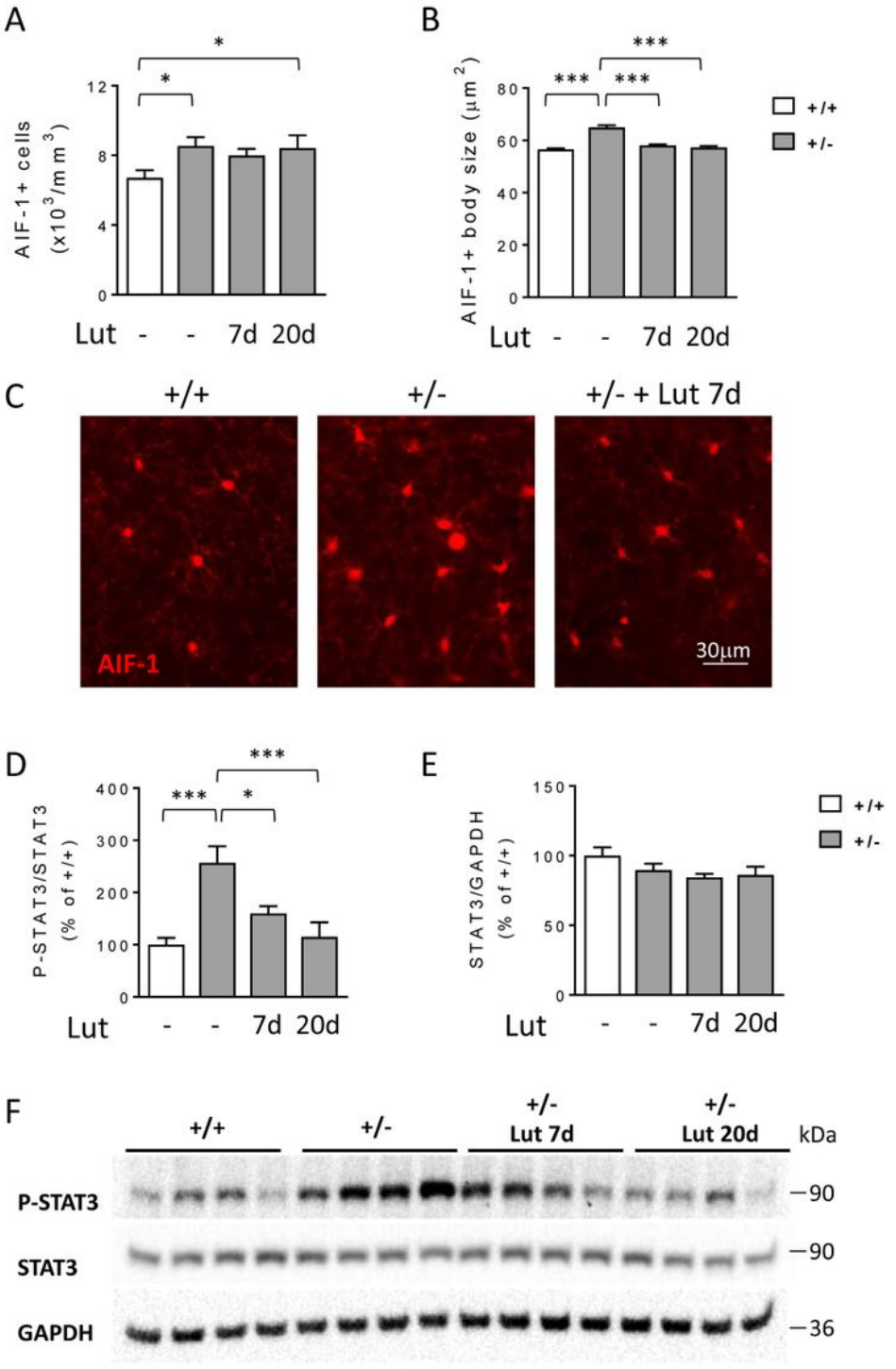

Figure 4

Effects of luteolin treatment on microglia activation in Cdkl5 +/- mice. A: Quantification of AIF-1-positive cells in somatosensory cortex from 3-month-old Cdkl5 +/+ (n=5) and Cdkl5 +/- (n=6) mice, and Cdkl5 +/- mice daily treated with luteolin intraperitoneal injections (i.p. 10 mg/Kg) for 7 (Lut 7d, n=4) or 20 days (Lut 20d, n=4). B: Mean AIF-1-cell body size of microglial cells in Cdkl5 female mice as in A. C: Representative fluorescence images of cortical sections processed for AIF-1 immunohistochemistry of a

Cdkl5 +/+ and a Cdkl5 +/- mouse, and a seven-day luteolin-treated Cdkl5 +/- mouse (+ Lut 7d). Values in A,B are represented as mean ± SEM. *p<0.05; ***p<0.001 (Fisher's LSD test after one-way ANOVA). D,E: Western blot analysis of P-STAT3 (Tyr 705), STAT3, and GAPDH levels in somatosensory cortex homogenates from untreated Cdkl5 mice (+/+ n=4, +/- n=4) and luteolin-treated Cdkl5 +/- mice as in A. Histograms show P-STAT3 (Tyr 705) protein levels normalized to corresponding total STAT3 protein levels in (D), and STAT3 levels normalized to GAPDH in (E). Data are expressed as percentages of Cdkl5 +/+ mice. Values are represented as means ± SEM of two independent experiments; *p<0.05; ***p < 0.001 (Fisher's LSD test after one-way ANOVA). F: Example of immunoblots from 4 animals of each experimental group.

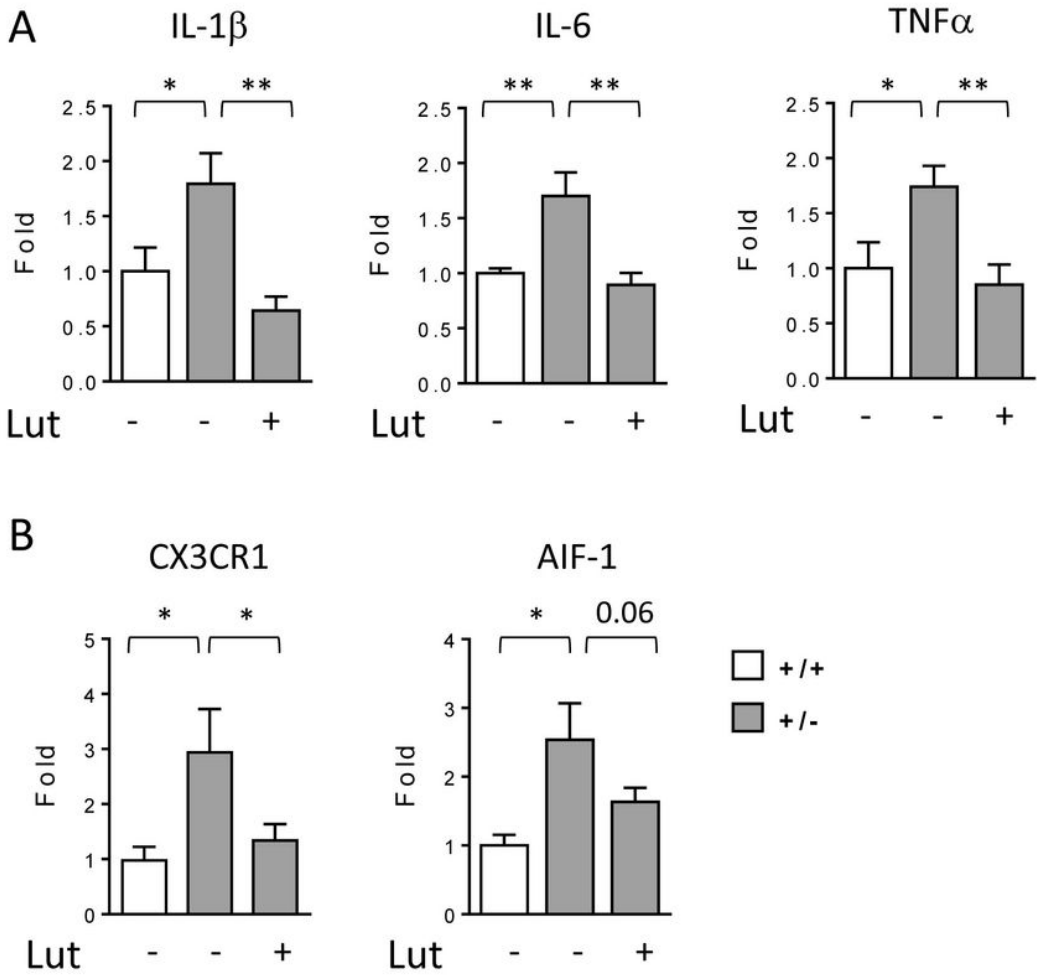

Figure 5

Effects of luteolin treatment on neuroinflammatory gene expression in microglial cells of Cdkl5 KO mice. A: Real-time qPCR analysis of Interleukin 1 beta (IL-1β Interleukin 6 (IL-6), and Tumor necrosis factor

alpha (TNFα) gene expression in microglial cells isolated from the brain of 3-month-old Cdkl5 +/+ (n=6) and Cdkl5 +/- (n=5) mice and 7-day luteolin-treated Cdkl5 +/- (n=6, Lut) mice. B: Expression of CX3C chemokine receptor 1 (CX3CR1) and Allograft inflammatory factor 1 (AIF-1) in microglial cells isolated from the brain of mice as in A. Data are given as fold change in comparison with microglial cells from Cdkl5 +/+ mice. * p<0.05; ** p<0.01; (Fisher's LSD test after one-way ANOVA).

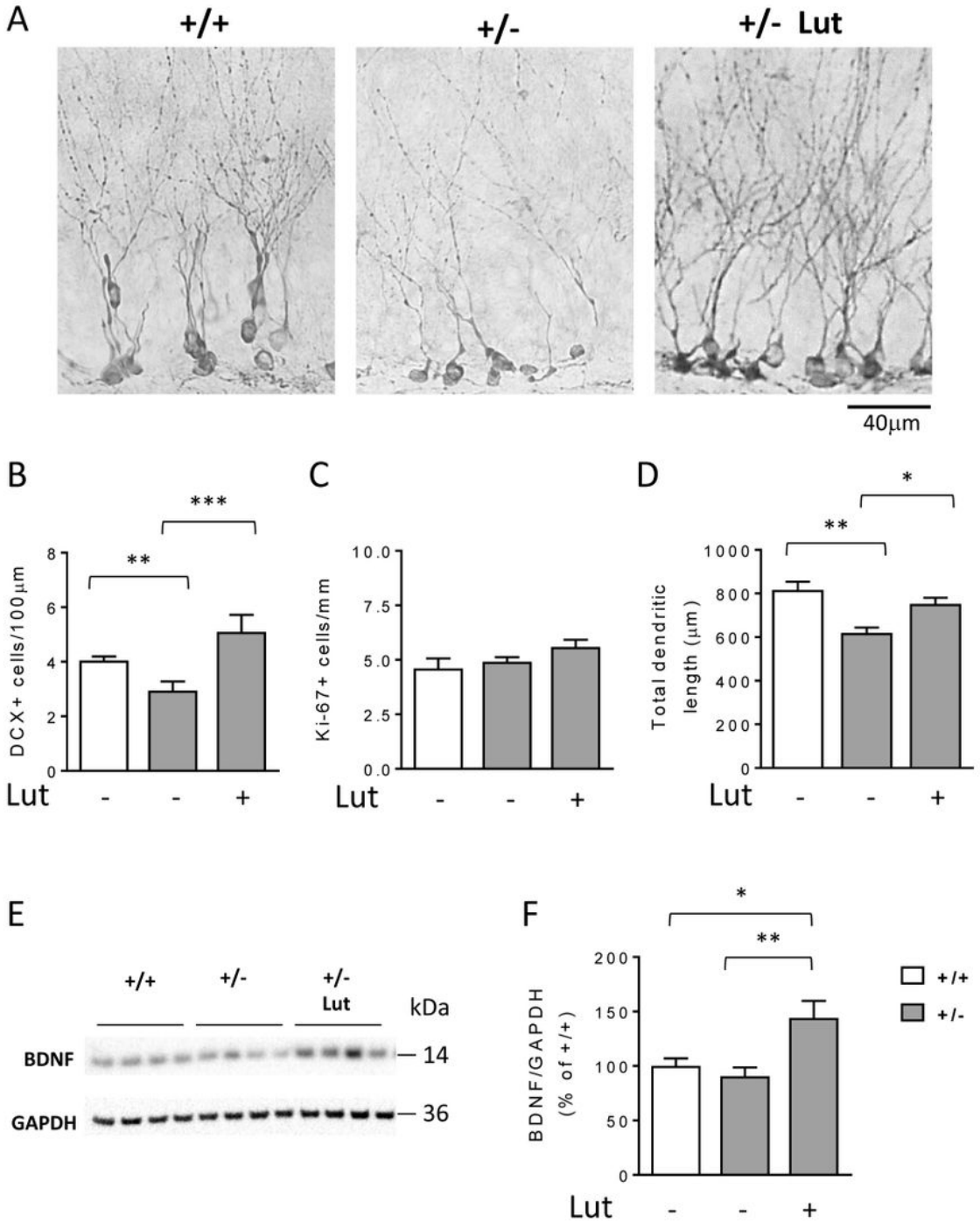

Figure 6

Effect of luteolin treatment on survival and maturation of postmitotic granule neurons in Cdkl5 KO mice. A: Examples of sections processed for DCX immunostaining from the dentate gyrus (DG) of an untreated WT (+/+), a heterozygous Cdkl5 KO female (+/-), and a 7-day luteolin-treated heterozygous Cdkl5 KO female (10 mg/Kg; +/- Lut 7d) mouse. B: Number of DCX-positive cells in the DG of treated Cdkl5 +/+ (n=6) and Cdkl5 +/- (n=6) mice, and Cdkl5 +/- 7-day luteolin-treated mice (Lut +, n=4). Data are expressed as number of DCX positive cells per 100 µm of granule cell layer. C: Number of Ki-67 positive cells in the DG of mice as in B. D: Mean total dendritic length of CA1 pyramidal neurons of mice as in B. Values in B,C and D are represented as means ± SEM. *P< 0.05, **P< 0.01 (Fisher's LSD test after one-way ANOVA). E,F: Western blot analysis of BDNF and GAPDH levels in somatosensory cortex homogenates from untreated Cdkl5 mice (+/+ n=4, +/- n=4) and 7-day luteolin-treated Cdkl5 +/- mice (+/-Lut7d, n=4) as in Fig. 4F. Examples of immunoblot in E. The nitrocellulose membrane used in the Western blot shown in Fig. 4F was probed with the anti-BDNF antibody. Histogram in F shows mature BDNF protein levels normalized to GAPDH. Data are expressed as a percentage of untreated Cdkl5 +/+ mice. Values are represented as means ± SEM of two independent experiments; *p<0.05;**p < 0.01 (Fisher's LSD test after one-way ANOVA).

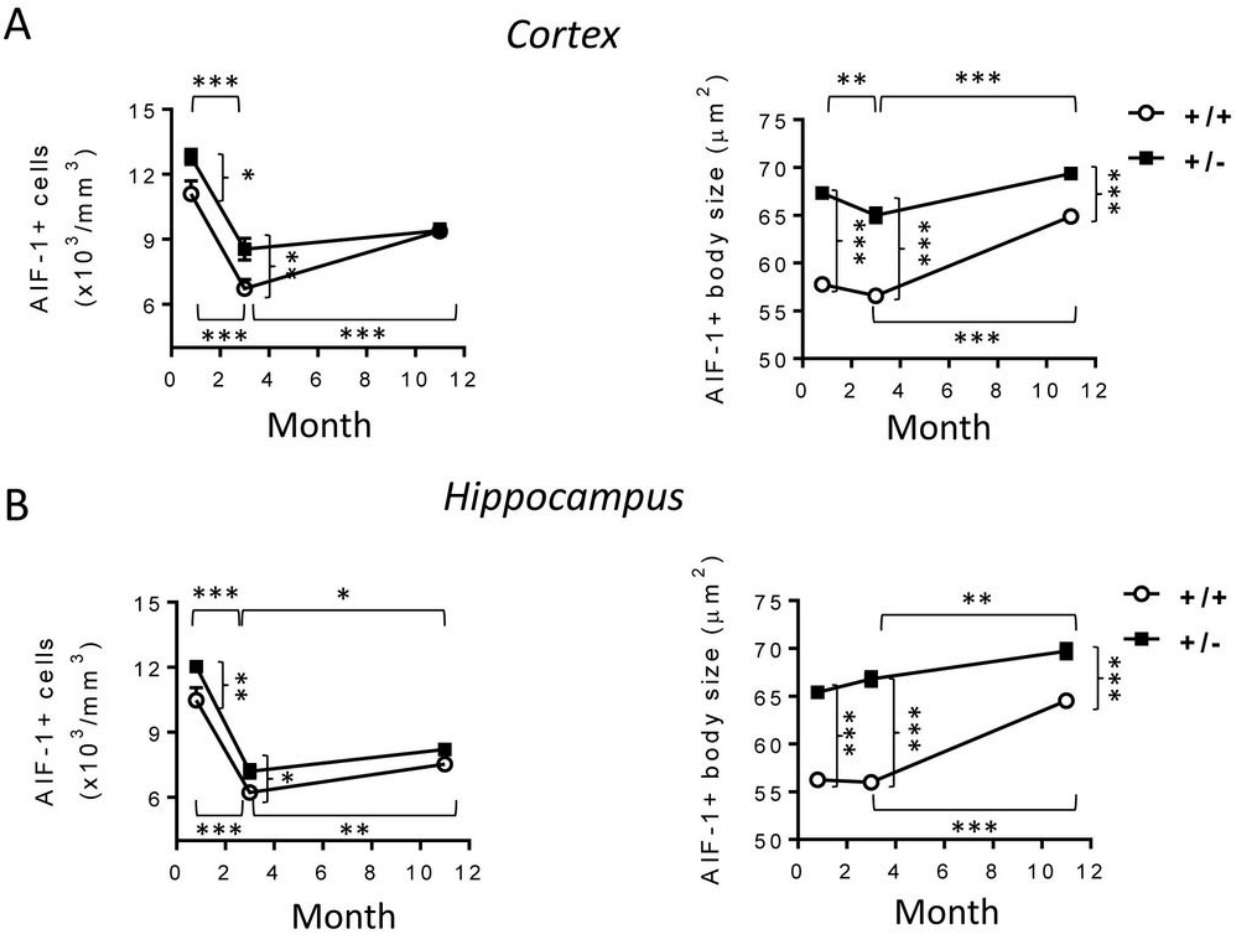

Figure 7

Assessment of microglia activation in different life stages of Cdkl5 +/- mice A,B: Quantification of the number of AIF-1-positive cells (on the left) and mean AIF-1-cell body size (on the right) of microglial cells in somatosensory cortex (A) and hippocampal sections (B) from young (20-day-old; +/+ n=5; +/- n=6), adult (3-month-old; +/+ n=5; +/- n=6), and middle-aged (11-month-old; +/+ n=4; +/- n=4) Cdkl5 mice. The results in A and B are presented as means ± SEM. * p<0.05; ** p<0.01; ***p<0.001 (Fisher's LSD test after two-way ANOVA).

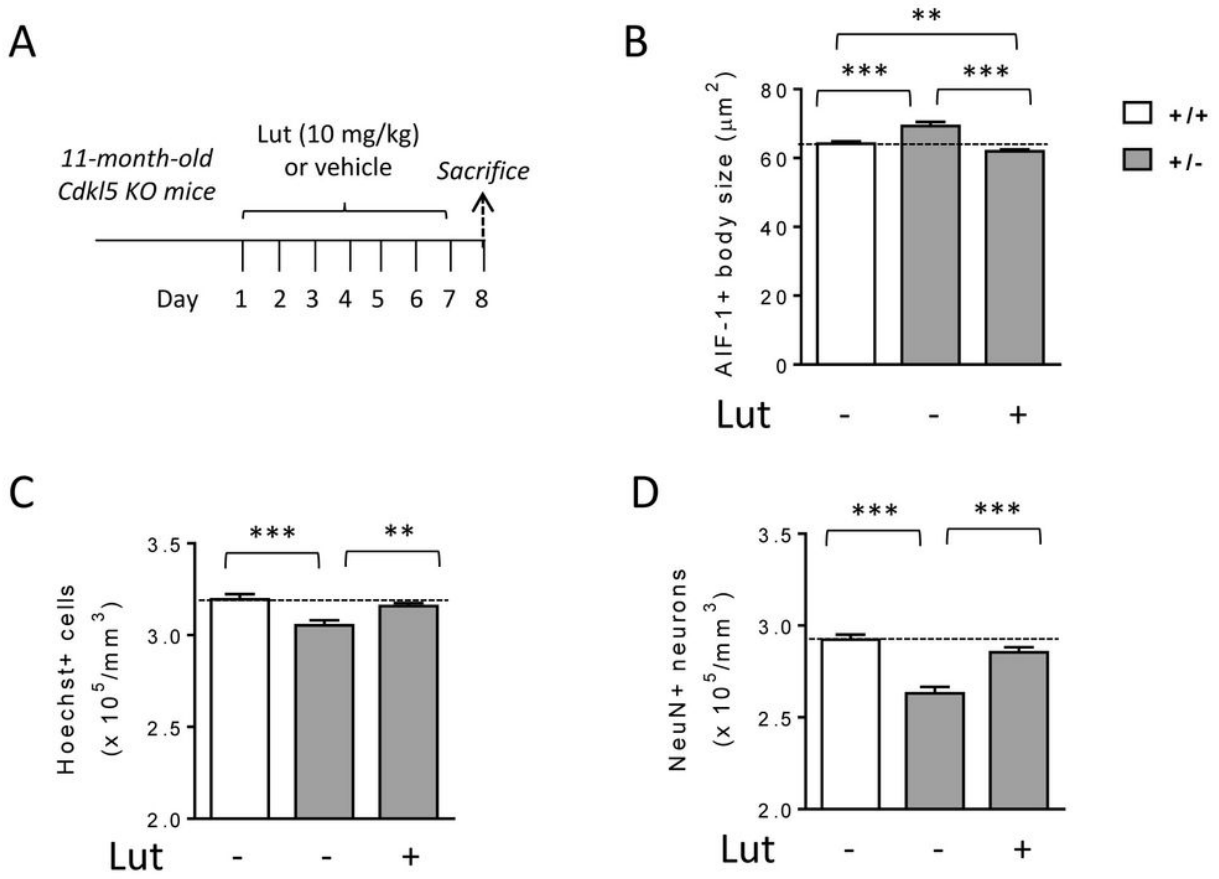

Figure 8

Effect of luteolin treatment in middle-aged Cdkl5 +/- mice. A: Schedule of treatment. Middle-aged (11-month-old) Cdkl5 mice were treated with vehicle or luteolin for 7 days. Mice were sacrificed 1 day after the end of treatment. B: Mean AIF-1-cell body size of microglial cells in the hippocampus of vehicle-treated (+/+ n=4; +/- n=4) and luteolin-treated (+/- n=4, Lut) middle-aged Cdkl5 mice. C,D: Quantification of Hoechst-positive cells (C), and NeuN positive cells (D) in CA1 layer of hippocampal sections from mice treated as in C. The results in B,C, and D are represented as means ± SEM. ** p<0.01; ***p<0.001 (Fisher's LSD test after one-way ANOVA).

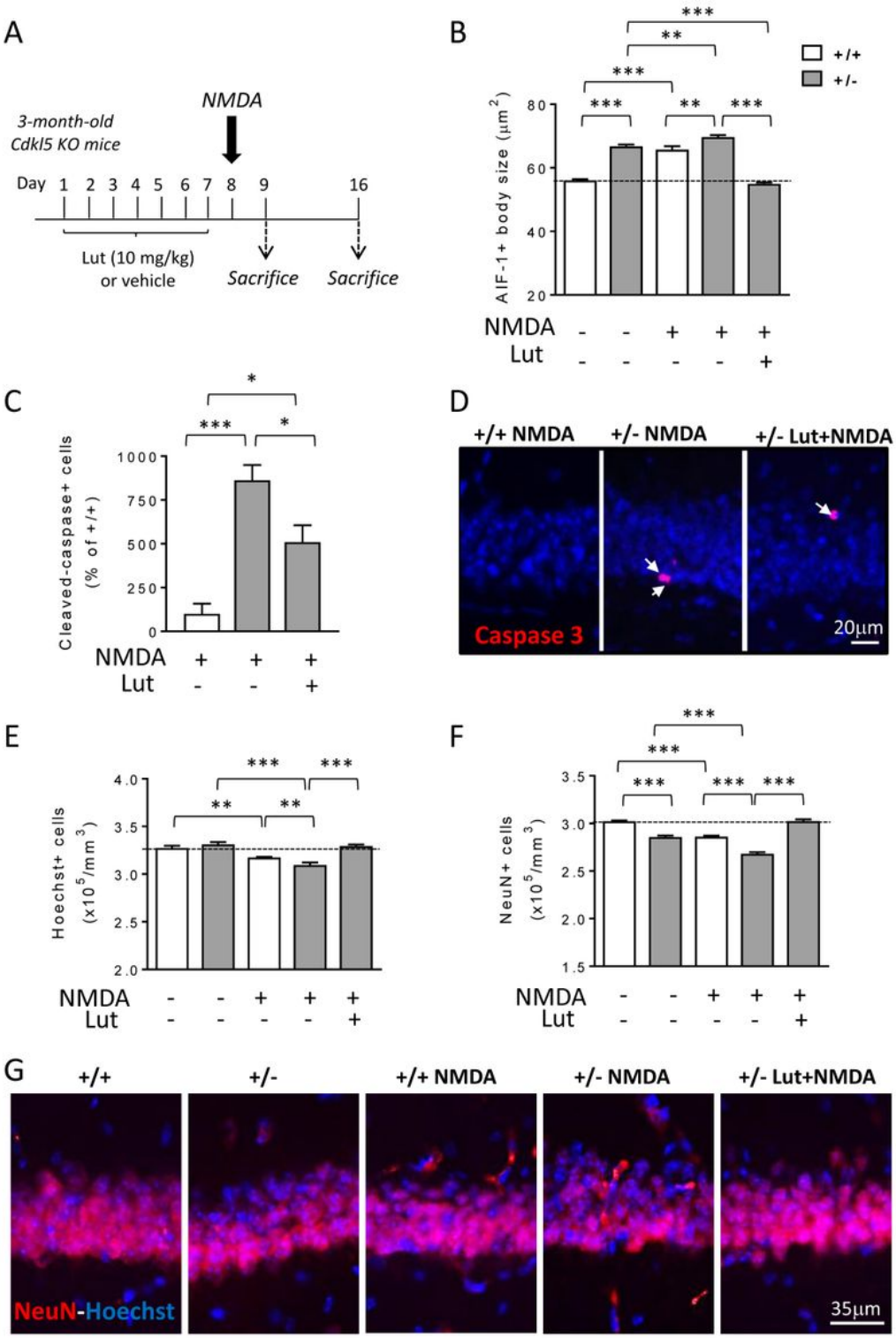

Figure 9

Effect of luteolin treatment on NMDA-induced excitotoxicity in the hippocampus of Cdkl5 +/- mice. A: Schematic view of in vivo treatments in 3-month-old Cdkl5 KO female mice. Mice received a single intraperitoneal injection of NMDA (60 mg/kg) after 7 days of vehicle or luteolin treatment. Animals were sacrificed 1 day or 8 days after NMDA administration. B: Mean AIF-1-cell body size of microglial cells in the hippocampus of Cdkl5 +/+ (n=5) and Cdkl5 +/- (n=6) mice treated with vehicle only, in Cdkl5 +/+

(n=3) and Cdkl5 +/- (n=3) mice treated with vehicle and NMDA and in Cdkl5 +/- (n=3) mice pre-treated for seven days with luteolin before NMDA injection. Mice were sacrificed 8 days after NMDA treatment. C: Number of cleaved caspase-3 positive cells in the hippocampus of Cdkl5 +/+ (n=3) and Cdkl5 +/- (n=4) mice treated with vehicle and NMDA, and in Cdkl5 +/- (n=6) mice pre-treated for 7 days with luteolin before NMDA injection. Mice were sacrificed 24 h after NMDA treatment. Data are given as a percentage of NMDA treated Cdkl5 +/+ mice. D: Examples of cleaved caspase-3 positive cells (white arrows) in CA1 layer of mice as in C. E,F: Quantification of Hoechst-positive cells (E), and NeuN positive cells (F) in CA1 layer of hippocampal sections from mice treated as in B. The results in B, E and F are presented as means ± SEM. * $p<0.05$; ** $p<0.01$; ***$p<0.001$ (Fisher's LSD test after one-way ANOVA). G: Representative fluorescent images of hippocampal sections of mice treated as in B immunostained for NeuN and counterstained with Hoechst.

Supplementary Files

This is a list of supplementary files associated with this preprint. Click to download.

- Additionalfile1.pdf
- GAPDH0.8.jpg
- GEL1E21.jpg
- GEL1E22.jpg
- GEL1E23.jpg
- GEL2E11.jpg
- LAB2021.jpg